Matter and Radiation at Extremes

RESEARCH ARTICLE

pubs.aip.org/aip/mre

Featured

Design of high-temperature superconductors at moderate pressures by alloying AlH_3 or GaH_3

Cite as: Matter Radiat. Extremes 9, 018401 (2024); doi: 10.1063/5.0159590
Submitted: 25 May 2023 • Accepted: 26 October 2023 •
Published Online: 1 December 2023

Xiaowei Liang,[1,2] Xudong Wei,[1] Eva Zurek,[3] Aitor Bergara,[4,5,6] Peifang Li,[7] Guoying Gao,[1,a)] and Yongjun Tian[1]

AFFILIATIONS

[1] Center for High Pressure Science (CHiPS), State Key Laboratory of Metastable Materials Science and Technology, Yanshan University, Qinhuangdao 066004, China
[2] School of Materials Science and Engineering, Henan University of Technology, Zhengzhou 450001, China
[3] Department of Chemistry, State University of New York at Buffalo, Buffalo, New York 14260-3000, USA
[4] Physics Department and EHU Quantum Center, University of the Basque Country, UPV/EHU, 48080 Bilbao, Spain
[5] Donostia International Physics Center (DIPC), 20018 Donostia, Spain
[6] Centro de Física de Materiales CFM, Centro Mixto CSIC-UPV/EHU, 20018 Donostia, Spain
[7] Extreme Conditions Physics Research Team, College of Physics and Electronic Information, Inner Mongolia Minzu University, Tongliao 028043, China

Note: Paper published as part of the Special Topic on High Pressure Science 2024.
[a)]**Author to whom correspondence should be addressed:** gaoguoying@ysu.edu.cn

ABSTRACT

Since the discovery of hydride superconductors, a significant challenge has been to reduce the pressure required for their stabilization. In this context, we propose that alloying could be an effective strategy to achieve this. We focus on a series of alloyed hydrides with the AMH_6 composition, which can be made via alloying A15 AH_3 (A = Al or Ga) with M (M = a group IIIB or IVB metal), and study their behavior under pressure. Seven of them are predicted to maintain the A15-type structure, similar to AH_3 under pressure, providing a platform for studying the effects of alloying on the stability and superconductivity of AH_3. Among these, the A15-type phases of $AlZrH_6$ and $AlHfH_6$ are found to be thermodynamically stable in the pressure ranges of 40–150 and 30–181 GPa, respectively. Furthermore, they remain dynamically stable at even lower pressures, as low as 13 GPa for $AlZrH_6$ and 6 GPa for $AlHfH_6$. These pressures are significantly lower than that required for stabilizing A15 AlH_3. Additionally, the introduction of Zr or Hf increases the electronic density of states at the Fermi level compared with AlH_3. This enhancement leads to higher critical temperatures (T_c) of 75 and 76 K for $AlZrH_6$ and $AlHfH_6$ at 20 and 10 GPa, respectively. In the case of $GaMH_6$ alloys, where M represents Sc, Ti, Zr, or Hf, these metals reinforce the stability of the A15-type structure and reduce the lowest thermodynamically stable pressure for GaH_3 from 160 GPa to 116, 95, 80, and 85 GPa, respectively. Particularly noteworthy are the A15-type $GaMH_6$ alloys, which remain dynamically stable at low pressures of 97, 28, 5, and 6 GPa, simultaneously exhibiting high T_c of 88, 39, 70, and 49 K at 100, 35, 10, and 10 GPa, respectively. Overall, these findings enrich the family of A15-type superconductors and provide insights for the future exploration of high-temperature hydride superconductors that can be stabilized at lower pressures.

I. INTRODUCTION

In recent years, hydrides have emerged as potential materials in the search of room-temperature superconductivity, not only from theoretical predictions[1–5] but also from experimental verifications.[6–22] In 2015, the predicted cubic H_3S was synthesized for the first time and was experimentally confirmed to have a T_c of 203 K at 155 GPa.[7,8] Four years later, the T_c record passed to the LaH_{10} metal hydride, with an H-clathrate structure, which was observed to have T_c values of 250–260 K at 170–190 GPa.[9,10]

Metallic clathrate hydrides were predicted to be a large class,[23–28] and some of the predictions of superconductivity in this family have been successively verified experimentally, such as for $ThH_{9/10}$ (146/161 K at 170–175 GPa),[11] YH_6 (224 K at 166 GPa and 220 K at 183 GPa),[12,13] YH_9 (243 K at 201 GPa and 262 K at 182 GPa),[13,14] and CaH_6 (215 K at 172 GPa and 210 K at 160 GPa).[15,16] These achievements have greatly encouraged the exploration of room-temperature superconductivity in hydrides.

However, the possible application of superconducting hydrides is not only influenced by the superconducting transition temperature, as in the case of other superconductors, but also by the stabilization pressure. Although the hydrides mentioned above have high T_c values, the pressures required to stabilize them are also extremely high (>150 GPa). Therefore, it is essential to obtain superconducting hydrides that are stable at low pressures. Our previous study proposed that the introduction of light B into the La–H system should lead to a stable $Fm\bar{3}m$ $LaBH_8$ phase with BH_8 units[29–31] that remains dynamically stable at 55 GPa and exhibits a T_c of 155 K. Subsequently, some other B-, C-, and Si-based ternary hydrides were also estimated to show good superconductivity at moderate pressures.[32–35] In these hydrides, the covalent units formed by including light elements with H contribute significantly to their low-pressure stability. Furthermore, an La–Y alloy tetrahydride was synthesized at 110 GPa, exhibiting a T_c of 92 K, and it can be recovered at 80 GPa, both of which are lower pressure thresholds than those required for the synthesis of YH_4.[18] Bi *et al.*[19] synthesized an (La,Ce)H_9 alloy at megabar pressures of 97–172 GPa, which exhibited a T_c of 148–178 K. More recently, the metastable compound $P6_3/mmc$-LaH_{10} was stabilized at 146 GPa by introducing Al atoms to form $P6_3/mmc$-(La,Al)H_{10}, with a T_c of 178 K.[20] An increase in the configurational entropy of a mixed alloy hydride will decrease its Gibbs free energy and enhance its stability. Therefore, alloying binary metal hydrides may be an alternative approach to optimize the stabilization pressure of superconducting hydrides.

Trihydrides are commonly found in binary metal hydrides, and their superconductivity under pressure has been extensively studied.[36–45] On the basis of their structures, common metal trihydrides can be divided into two categories, one with the $Pm\bar{3}n$ structure and the other with the $Fm\bar{3}m$ structure. This provides a platform to tune the stability and superconductivity of hydrides by alloying. The $Pm\bar{3}n$ structure, also called the A15 structure, is well known for its excellent superconducting performance. To date, about 50 alloys with this structure have been found to be superconductors, and some of them remain the most promising materials for practical applications.[46] Among binary hydrides, AlH_3, GaH_3, ZrH_3, and HfH_3 were predicted to become stable in the A15 structure at 73, 160, 8, and 27 GPa, respectively, with the metal atoms forming a body-centered cubic (bcc) lattice and the six H atoms occupying half of the tetrahedral interstices of this lattice.[36–40] Interestingly, the A15 phases of AlH_3 and ZrH_3 were confirmed in experiments at 100 and 30 GPa, respectively, but they do not exhibit high T_c values.[37,39,41] On the other hand, the Al5 phase of GaH_3 was estimated to have the highest T_c of 102 K at 120 GPa.[38] However, A15 GaH_3 requires relatively high minimum pressures of ~160 and ~84 GPa for thermodynamic and dynamic stability respectively,[38,47] making its synthesis difficult. Below 160 GPa, A15 GaH_3 becomes thermodynamically unstable and transforms into a structure containing H_2 units, with an insulating character.[26] Compared with Al and Ga, group IIIB and IVB metal atoms are less electronegative and could transfer more electrons to H_2 units, allowing structures with atomic hydrogen to remain stable at lower pressures. In addition, group IIIB and IVB metals can also exist in the trivalent state and form trihydrides. Therefore, alloying AlH_3/GaH_3 with group IIIB/IVB metals could give stable alloy hydrides with an A15-type structure and the expected superconductivity at low pressures. For ternary hydrides, A15-type $GaAsH_6$ and $YZrH_6$ were predicted to have T_c values of 98 and 16 K at 180 GPa and ambient pressure, respectively.[28,48] Recently, our group designed a series of A15-type ternary hydrides, with the $CaSnH_6$ alloy demonstrating the lowest thermodynamically stable pressure of 110 GPa and $CaSnH_6$ with the lowest dynamically stable pressure of 41 GPa,[47] which also facilitated our exploration of ternary alloy hydrides. To some extent, alloying AlH_3/GaH_3 with group IIIB/IVB metals also provides a way to control the physical properties of ternary hydrides through the choice of their constituent elements.

In this work, we investigate theoretically the structure, stability, and superconductivity of alloy hydrides with the AMH_6 composition (A = Al or Ga; M = a group IIIB or IVB metals). We chose the AMH_6 composition because the substitution of an M atom for an A atom in the A_2H_6 unit cell is one of the most intuitive ways to form alloy hydrides. Furthermore, considering the promoting effect of configurational entropy in material formation, mixing metal elements in equal proportions may yield a highly disordered alloy hydride, making it more favorable for experimental synthesis. The results show that seven ternary hydrides, $AlMH_6$ (M = Ti, Zr, or Hf) and $GaMH_6$ (M = Sc, Ti, Zr, or Hf) are identified to be stable in the A15-type structure. A15-type $AlZrH_6$, $AlHfH_6$, and $GaMH_6$ for all M are thermodynamically stable at pressures much lower than those required to stabilize A15 AlH_3 and GaH_3. Except for $GaScH_6$, all of these hydrides also have significant advantages over AlH_3 and GaH_3 in terms of the lowest dynamically stable pressures, with $AlZrH_6$, $AlHfH_6$, $GaZrH_6$, and $GaHfH_6$ able to maintain their dynamical stability at ~13, 6, 5, and 6 GPa, respectively. Electron–phonon coupling (EPC) calculations show that all of these ternary hydrides are superconducting. Among them, the estimated T_c values for $AlZrH_6$, $AlHfH_6$, $GaScH_6$, $GaZrH_6$, and $GaHfH_6$ are 75, 76, 88, 70, and 49 K at 20, 10, 100, 10, and 10 GPa, respectively. In addition, $AlScH_6$ and $AlYH_6$ are predicted to be stable in structures similar to $Fm\bar{3}m$ Sc(Y)H_3, and they are also potential superconductors under pressure. Our results indicate that they have great potential for the exploration of low-pressure stable high-T_c superconductors in alloy hydrides.

II. COMPUTATIONAL DETAILS

Structure searches of AMH_6 with simulation cells containing up to four formula units were performed at 50–300 GPa by using the particle swarm optimization technique implemented in the CALYPSO code.[49,50] Structural relaxations and calculations of electronic properties were performed using the Vienna *Ab Initio* Simulation Package (VASP) code based on density functional theory (DFT) with the Perdew–Burke–Ernzerhof generalized gradient approximation.[51,52] The ion–electron interaction was described by projector-augmented-wave potentials, with $1s^1$, $3s^23p^1$, $3d^{10}4s^24p^1$, $3s^23p^63d^14s^2$, $4s^24p^64d^15s^2$, $5s^25p^65d^16s^2$, $3s^23p^63d^24s^2$,

$4s^2 4p^6 4d^2 5s^2$, and $5p^6 5d^2 6s^2$ configurations being treated as valence electrons for H, Al, Ga, Sc, Y, La, Ti, Zr, and Hf atoms, respectively.[53] The plane-wave kinetic energy cutoff was set to 700 eV, and the corresponding Monkhorst–Pack (MP) k-point meshes were adopted for different structures to ensure that enthalpy converged to 1 meV/atom. Phonon calculations were performed using the PHONOPY[54] or Quantum-ESPRESSO codes.[55] EPC calculations of $Pm\bar{3}$ ternary hydrides were carried out with the Quantum-ESPRESSO code using ultrasoft pseudopotentials for all the atoms. A $9 \times 9 \times 9$ q-point mesh in the first Brillouin zone (BZ) was used in the EPC calculation, and an MP grid of $36 \times 36 \times 36$ was considered, to ensure k-point sampling convergence.

III. RESULTS AND DISCUSSION

We performed structure searches for 12 ternary hydrides with the AMH_6 composition in the pressure range of 50–300 GPa. Seven hydrides ($AlTiH_6$, $AlZrH_6$, $AlHfH_6$, $GaScH_6$, $GaTiH_6$, $GaZrH_6$, and $GaHfH_6$) were identified as having an A15-type structure with the $Pm\bar{3}$ symmetry, as shown in Fig. 1(a). In this structure, two metal atoms occupy the vertex and the center positions to form a bcc lattice, with H atoms occupying locations near their tetrahedral interstices. The A–H, M–H, and H–H bond distances for $Pm\bar{3}$ AMH_6 at 100 GPa are shown in Table S1 (supplementary material). The A–H distance is shorter than the M–H distance in $AlZrH_6$ and $AlHfH_6$, while the reverse happens in $AlTiH_6$ and $GaMH_6$. Different metal atoms in the structure lead to two different lengths between adjacent H atoms. The calculated H–H distances of 1.45–1.75 Å are much longer than those of 0.74 and 1.2 Å in H_2 and LaH_{10} at 100 GPa, respectively, indicating that H atoms are not bonded to each other. Except for $GaTiH_6$ and $GaScH_6$, the other five hydrides have no phase transition in the entire pressure range from 50 to 300 GPa. For $GaTiH_6$ and $GaScH_6$, the $C2/m$ and $Pmma$ structures, respectively, were predicted to be stable at 50 GPa, and they do not present H_2 molecules in their structures (Fig. S1, supplementary material). Furthermore, $AlScH_6$ and $AlYH_6$ were predicted to have structures similar to $Fm\bar{3}m$ $Sc(Y)H_3$, where metal atoms form a face-centered cubic (fcc) lattice and H atoms are located at the tetrahedral and octahedral interstices of this lattice. As shown in Fig. S2 (supplementary material), $Pmmn$ $AlScH_6$ can be seen as a $2 \times 2 \times 1$ supercell of $Fm\bar{3}m$ $Sc(Y)H_3$ with two metal atoms arranged alternately in two directions. $P4/mmm$ $AlScH_6$ is formed by replacing the two Sc atoms in $Fm\bar{3}m$ ScH_3 with Al atoms. $I4/mmm$ $AlYH_6$ is similar to $P4/mmm$ $AlScH_6$, but with slightly shifted H positions. The predicted structures of $AlLaH_6$, $GaYH_6$ and $GaLaH_6$ are also shown in Fig. S3 (supplementary material).

Bader charge analyses[56] were performed on A15-type ternary hydrides at 100 GPa, as shown in Table S2 (supplementary material). The results demonstrate the transfer of electronic charges from metal to H atoms, suggesting an ionic nature of the bonding between them. Each H atom in $AlMH_6$ and $GaMH_6$ accepts ~0.60–0.64 and 0.39–0.43e, respectively. In $AlMH_6$, Al atoms transfer around 2.31–2.71e to H atoms, surpassing the ~1.31 to 1.54e transferred from the M atoms. In $GaMH_6$, the M atom loses a greater amount

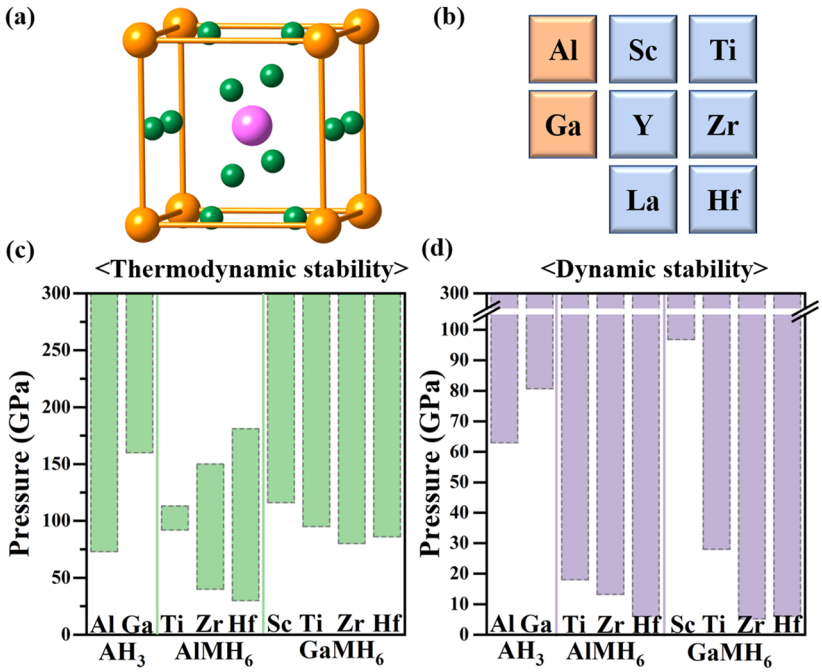

FIG. 1. (a) Crystal structure of the A15-type ternary hydrides. Orange, magenta, and green balls represent A (Al or Ga), M (a group IIIB or IVB metal), and H atoms, respectively. (b) Elements considered for the ternary hydrides. (c) Thermodynamic and (d) dynamical stability phase diagrams of the $Pm\bar{3}$ hydrides with pressure.

of charge (~1.34 to 1.61e) compared with the Ga atom (~0.94 to 1.00e), indicating a greater ionic nature of the M–H bond. The electrons acquired by the H_2 molecule occupy its antibonding orbitals, leading to an elongation of the H–H bond length and potentially even dissociation of the H_2 unit. In $AlMH_6$, the significant electron transfer from Al to H atoms compensates for the relatively smaller electrons transfer from the M atom. In contrast to GaH_3, the doping M atoms enable H atoms to gain more charge in $GaMH_6$ at the same pressure, thereby allowing these ternary hydrides to exhibit structures with atomic H at lower pressures. Additionally, the electron localization functions (ELFs) were calculated for these A15 ternary hydrides at 100 GPa with an isosurface value of 0.5, as depicted in Fig. S4 (supplementary material). The ELFs indicate that electrons are predominantly localized around the H atoms, confirming their role as electron acceptors. The ELF values below 0.5 between adjacent H atoms indicate the absence of H–H covalent bonds. The ELF values between the metal and H atoms approach zero, confirming their ionic bonding character, which is consistent with the aforementioned Bader charge analysis.

The thermodynamic stability of these ternary hydrides has been assessed by calculating their formation enthalpies relative to elemental solids and binary compounds.[36,38–40,42–45] The relative enthalpy curves for AMH_6 are presented in Fig. 2 and Fig. S5 (supplementary material). The calculations consider the most stable configuration for each component, and the total energy of AH_3 and MH_3 is used as the reference energy. Within certain pressure ranges, AMH_6 exhibits lower formation enthalpy compared with possible decomposition pathways, indicating that AMH_6 is thermodynamically stable. For $AlMH_6$ (M = Ti, Zr, or Hf), the predicted A15-type phases remain stable within the pressure ranges of 78–165, 69–123, and 43–157 GPa, respectively. On accounting for zero-point energy (ZPE), the stable pressure range for $AlTiH_6$ shrinks to 92–113 GPa and the relative formation enthalpy reduces to only −10 meV/f.u. Conversely, with ZPE corrections, the stable pressure ranges for $AlZrH_6$ and $AlHfH_6$ expand to 40–150 and 30–181 GPa, respectively. Furthermore, the stability pressure thresholds for both hydrides are lower than the 73 GPa threshold for AlH_3[36] [Fig. 1(c)]. Regarding $GaMH_6$ (M = Sc, Ti, Zr, or Hf), the predicted A15-type phases are stable above 126, 96, 85, and 95 GPa, respectively, and remain stable with increasing pressure. With ZPE taken into account, the minimal stable pressures change to 116, 95, 80, and 86 GPa, respectively, which are well below the stability threshold of 160 GPa for GaH_3 [Fig. 1(c)]. Therefore, it is anticipated that the experimental synthesis of A15-type $GaMH_6$ might be easier compared with that of GaH_3. Inspired by the successful synthesis of the equal-atomic $(La,Y)H_4$ and $(La,Ce)H_9$ alloys, the high-temperature and high-pressure reaction of AM alloys with NH_3BH_3 might be a promising route for the synthesis of the alloys AMH_6.[18,19] Figure S5 (supplementary material) demonstrates that the $Fm\bar{3}m$-like $AlScH_6$ is stable above 150 GPa and undergoes a transformation from the

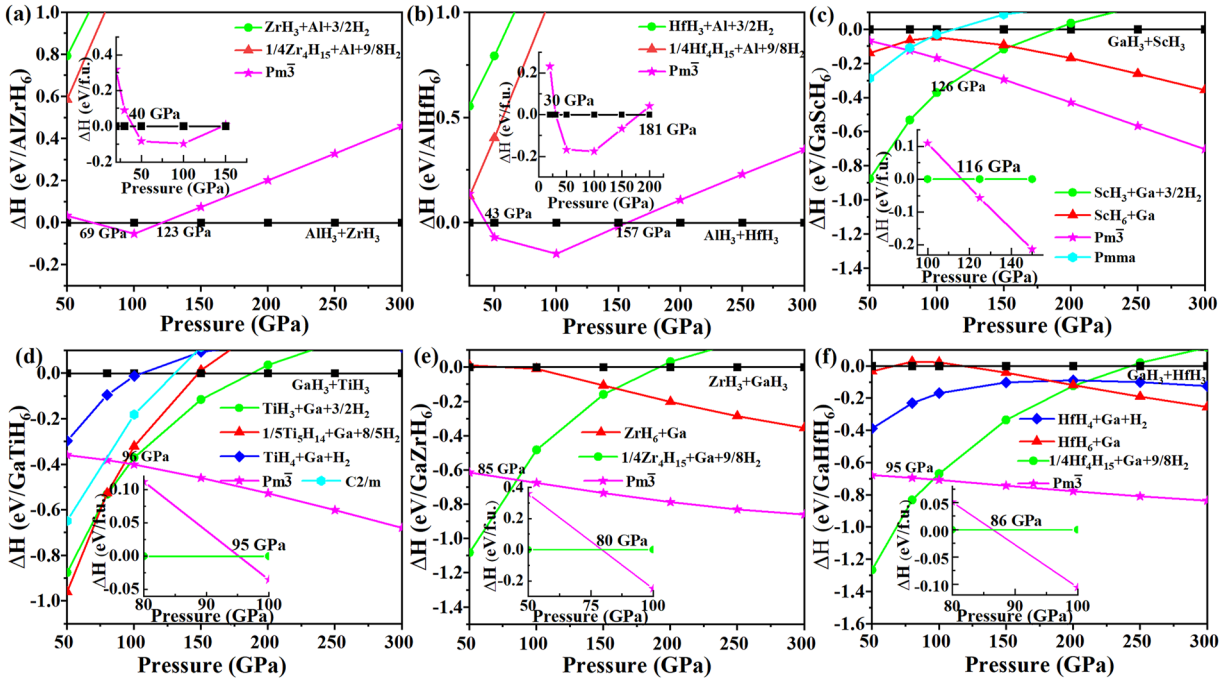

FIG. 2. Relative enthalpy curves of predicted structures for (a) $AlZrH_6$, (b) $AlHfH_6$, (c) $GaScH_6$, (d) $GaTiH_6$, (e) $GaZrH_6$, and (f) $GaHfH_6$ with respect to AH_3 (A = Al and Ga) and MH_3 (M = Sc, Ti, Zr, and Hf) under pressure. The insets show the relative enthalpies with ZPE taken into account. The following structures for the elemental solids and binary hydrides were used for the ΔH calculations: $P6_3/m$, $C2/c$, and $Cmca$ for H_2; $Fm\bar{3}m$ and $P6_3/mmc$ for Al; $Fm\bar{3}m$ for Ga; $R\bar{3}c$, $Pnma$, and $Pm\bar{3}n$ for AlH_3; $P2_1/m$ and $Pm\bar{3}n$ for GaH_3; $Pm\bar{3}n$ and $R\bar{3}c$ for ZrH_3; $I\bar{4}3d$ for Zr_4H_{15}; $Cmc2_1$ and $I4/mmm$ for ZrH_6; $Pm\bar{3}n$ for HfH_3; $I\bar{4}3d$ for Hf_4H_{15}; $Cmc2_1$ for HfH_6; $Fm\bar{3}m$ for ScH_3; $Cmcm$, $P6_3/mmc$, and $Im\bar{3}m$ for ScH_6; $Fm\bar{3}m$ for TiH_3; $I\bar{4}$ for Ti_5H_{14}; $Fddd$ for TiH_4.

Pmmn phase to the *P*4/*mmm* phase at 318 GPa. The *C*2/*m* phase of $AlYH_6$ is stable above 45 GPa and transforms to the $Fm\bar{3}m$-like *I*4/*mmm* phase at 115 GPa. $AlLaH_6$ is predicted to exhibit the $P6_3/mmc$ and *Cmcm* structures below ~200 GPa. For $GaYH_6$ and $GaLaH_6$, the low-symmetry $P2_12_12$ and *C*2/*m* structures are stable near 100 GPa and below 150 GPa, respectively. Additionally, we also performed structure predictions and first-principles calculations for hydrides with higher H content in the Al–Zr–H, Ga–Sc–H, Ga–Zr–H, and Ga–Hf–H systems at 200 and 300 GPa. As shown in Fig. S6 (supplementary material), these H-rich hydrides have higher formation enthalpies relative to AH_3+ BH_3 + H_2 or AMH_6 + H_2, indicating that they are unstable at the corresponding pressures.

To better understand why the A15-type AMH_6 structure is stable, we conducted an analysis of the influence of the relative internal energy (ΔU) and the product of pressure and volume (ΔPV) on the relative enthalpy (ΔH) under pressure. The findings for $AlZrH_6$ and $AlHfH_6$ are illustrated in Fig. S7 (supplementary material). As pressure increases, the ΔPV term also rises and eventually exhibits positive values. Conversely, the ΔU term exhibits the opposite trend, indicating that the bonding in both ternary hydrides contributes significantly to their stabilization. For the A15-type $GaMH_6$ (Fig. S8, supplementary material), the ΔPV contribution in all four hydrides is negative in comparison with the benchmark, indicating that the ΔPV term plays a dominant role in their thermodynamic stability. Meanwhile, the magnitude of ΔU decreases with increasing pressure, leading to an overall enhancement of the stability of these ternary hydrides. Furthermore, in $GaScH_6$, the ΔPV and ΔU terms exhibit contrasting trends when compared with ScH_3 + GaH_3. The negative ΔPV contribution counteracts the negative effect of the ΔU term, ultimately resulting in the stabilization of $GaScH_6$. Both the ΔPV and ΔU contribution in $GaTiH_6$, $GaZrH_6$,

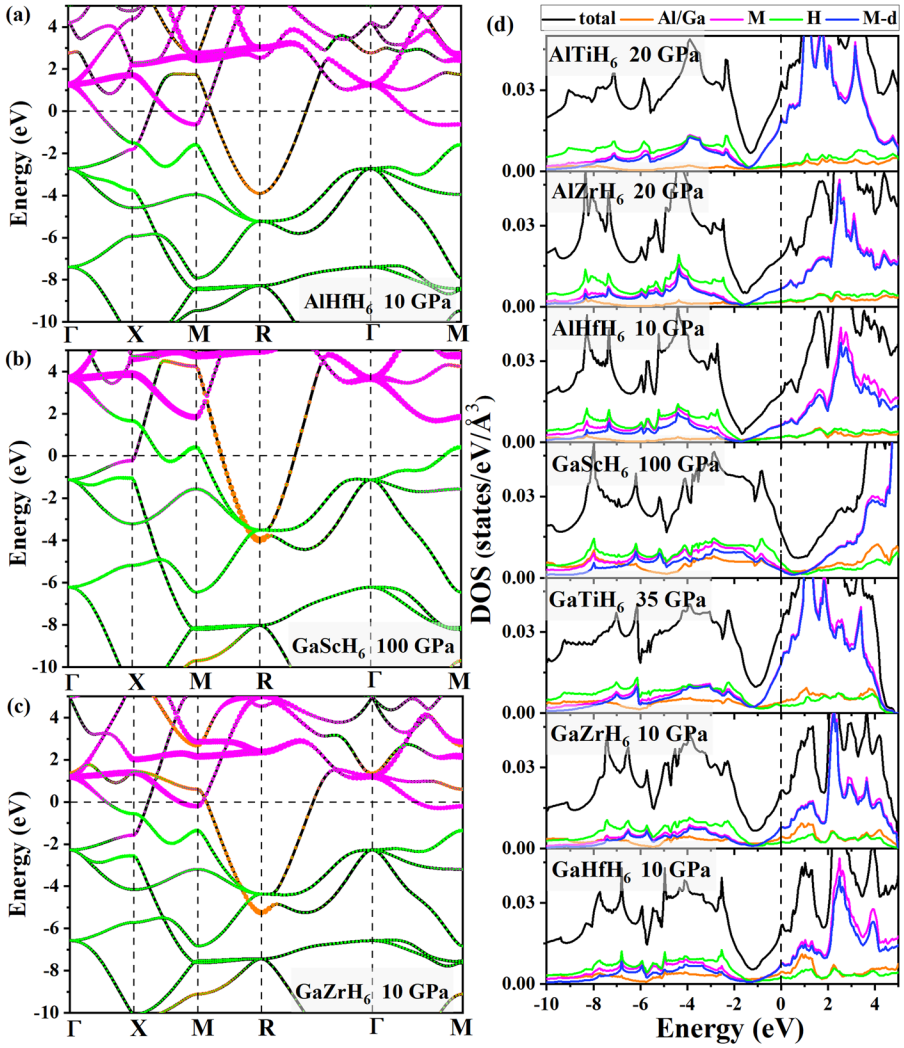

FIG. 3. Calculated band structures and electronic DOS of $Pm\bar{3}$ ternary hydrides at different pressures.

and $GaHfH_6$ have favorable effects on thermodynamic stability compared with their respective binary hydrides.

We also investigated the dynamical stability of the predicted A15-type AMH_6 compounds by calculating the phonon spectra using the supercell approach implemented in the PHONOPY code[54] (Figs. S14 and S15, supplementary material). Within their respective thermodynamically stable pressure ranges, no imaginary frequencies were observed in the phonon spectra of these compounds, indicating their dynamical stability. Furthermore, we systematically explored the minimum pressure required for dynamical stability of these A15-type AMH_6. As pressure decreases, phonon softening begins to occur, eventually leading to instability with the appearance of imaginary frequencies at certain q-wave vectors. We plotted the evolution of the frequency with pressure at the q-wave vector where the largest imaginary frequency occurs. As depicted in Figs. S9 and S10 (supplementary material), A15-type $GaScH_6$ exhibited the highest critical pressure for dynamical stability, estimated to be around 97 GPa. $GaTiH_6$ followed, with a critical pressure of ~28 GPa. $AlTiH_6$ and $AlZrH_6$ were found to be dynamically stable at lower pressures of about 18 and 13 GPa, respectively. Interestingly, the critical pressures for dynamical stability of $AlHfH_6$, $GaZrH_6$, and $GaHfH_6$ were considerably lower, at around 6, 5, and 6 GPa, respectively. Moreover, the threshold pressures for dynamical stability of the five ternary hydrides ($GaTiH_6$, $AlTiH_6$, $AlHfH_6$, $GaZrH_6$, and

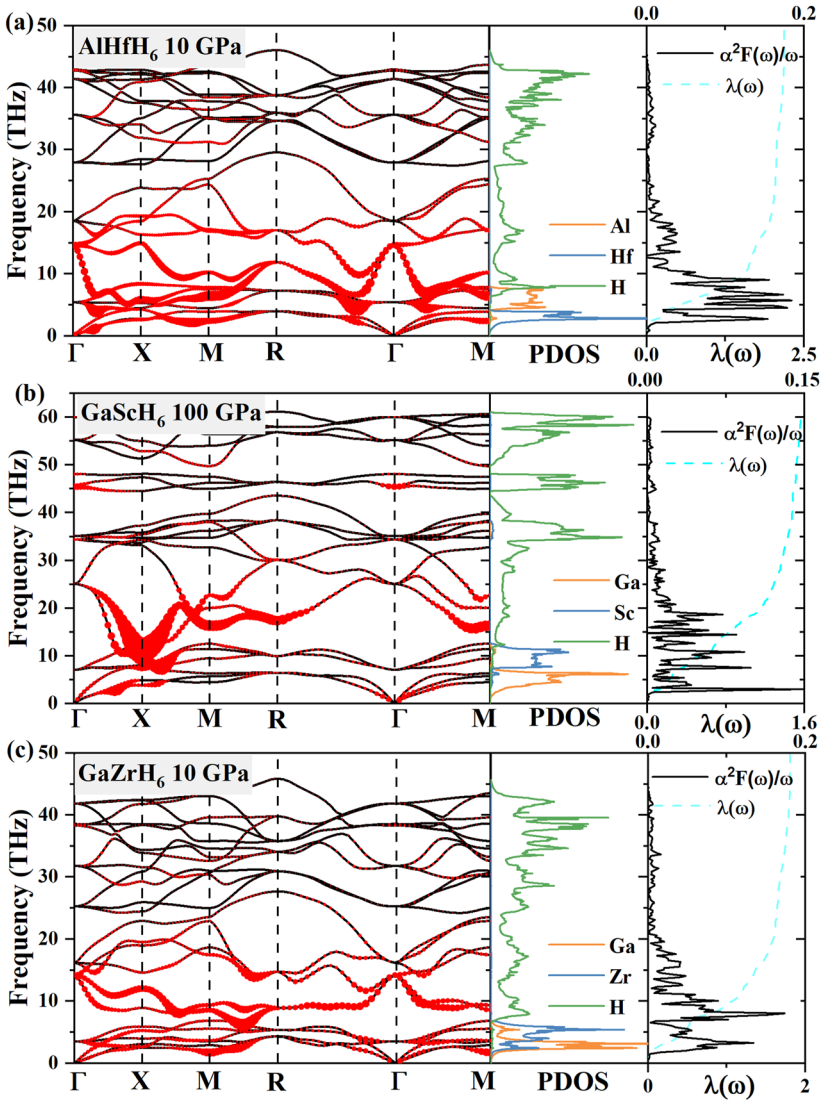

FIG. 4. Calculated phonon dispersion curves (the area of the red circles is proportional to the EPC strength), projected phonon density of states (PDOS), Eliashberg phonon spectral function $\alpha^2F(\omega)/\omega$, and its integral $\lambda(\omega)$ for (a) $Pm\bar{3}$ $AlHfH_6$ at 10 GPa, (b) $Pm\bar{3}$ $GaScH_6$ at 100 GPa, and (c) $Pm\bar{3}$ $GaZrH_6$ at 10 GPa.

$GaHfH_6$) were much lower compared with those of AH_3 and MH_3 [Figs. S11 and S13 (supplementary material) and Fig. 1(d)]. This suggests that these ternary hydrides could potentially be recovered at lower pressures, provided that the barriers preventing them from decomposing are sufficiently high. Of the $Fm\bar{3}m$-like ternary hydrides, *Pmmn* $AlScH_6$, *P*4/*mmm* $AlScH_6$, and *I*4/*mmm* $AlYH_6$ could maintain their dynamical stability to 65, 139, and 43 GPa, respectively (Figs. S12 and S16, supplementary material).

The electronic properties of the predicted A15-type AMH_6 compounds were investigated at different pressures, and the results are displayed in Fig. 3, as well as Figs. S17 and S18 (supplementary material). The calculated density of states (DOS) reveals the presence of electronic states at the Fermi energy level (E_f), indicating that these hydrides exhibit metallic behavior within the studied pressure range. The contributions of the metal and hydrogen atoms to the total DOS are also depicted in the figures. Figure 3(d) highlights a distinct difference between the DOS of $GaScH_6$ and the other six hydrides composed of Al/Ga and group IVB metals. In $GaScH_6$, the hydrogen atoms contribute significantly to the DOS at E_f, suggesting the potential for excellent superconducting properties. In the remaining six hydrides, the group IVB metals have one additional valence electron compared with Sc atoms, causing a shift of E_f to higher energies relative to $GaScH_6$. These six hydrides exhibit higher or comparable total DOS at E_f compared with $GaScH_6$. However, the DOS contributions from Al and Ga atoms are lower owing to significant charge transfer to the H atoms. In the case of the group IVB metals, the DOS at E_f is mainly contributed by *d* orbitals. Furthermore, the electronic band structures of $AlHfH_6$, $GaScH_6$, and $GaZrH_6$ were examined as examples at pressures of 10, 100, and 10 GPa, respectively. The band projections onto different elements are also displayed in the band structures. In these three hydrides, a band associated with Al/Ga atoms is observed to cross E_f steeply along the M–R–Γ direction. Additionally, in $AlHfH_6$ and $GaZrH_6$ there is an electron pocket at the M point and a flat band along the Γ–M direction, dominated by Hf and Zr atoms, located near E_f. In the case of $GaScH_6$, electron and hole pockets are observed along the X–M direction, along with a flat band along the Γ–M direction, which are attributed to H atoms. These localized electronic states contribute to a high DOS at the Fermi energy and play a role in electron–phonon interactions. Moreover, a comparison was made between the DOS of A15-type AlH_3, $AlTiH_6$, $AlZrH_6$, and $AlHfH_6$ at 100 GPa. As shown in Fig. S17 (supplementary material), the DOS at E_f for $AlTiH_6$, $AlZrH_6$, and $AlHfH_6$ are 0.030, 0.018, and 0.018 states eV^{-1} $Å^{-3}$ respectively, which are significantly higher than that of AlH_3 (0.008 states eV^{-1} $Å^{-3}$). The doping of AlH_3 with Ti, Zr and Hf atoms elevated E_f, resulting in an increased DOS at E_f. Ternary hydrides exhibit a more pronounced metallic character compared with AlH_3, potentially enhancing their superconducting properties.

After determining the stability and metallicity of A15-type ternary hydrides, we conducted EPC calculations to investigate their superconductivity. The calculated phonon dispersion curves, projected phonon density of states (PDOS), Eliashberg phonon spectral function $\alpha^2F(\omega)/\omega$, and its integral $\lambda(\omega)$ for $Pm\bar{3}$ $AlHfH_6$, $GaScH_6$ and $GaZrH_6$ at pressures of 10, 100, and 10 GPa are displayed in Fig. 4. From the PDOS, it is evident that the high-frequency and low-frequency phonon modes are associated with the vibrations of H and metal atoms, respectively. The right-hand panels of Fig. 4 illustrate that the peaks of $\alpha^2F(\omega)/\omega$ for $AlHfH_6$, $GaScH_6$, and $GaZrH_6$ are predominantly distributed below 15, 20, and 15 THz, respectively, with the corresponding $\lambda(\omega)$ increasing rapidly. The EPC strength on the different phonon modes is also depicted on the phonon dispersions. As a result, the significant contribution to the EPC comes from the soft modes associated with H-atom vibrations and the modes dominated by metal atoms. This leads to a total EPC parameter λ of 2.18, 1.56, and 1.80 for $AlHfH_6$, $GaScH_6$, and $GaZrH_6$ at pressures of 10, 100, and 10 GPa, respectively.

The superconducting critical temperatures of the predicted A15-type ternary hydrides were calculated using the Allen–Dynes modified McMillan equation with a Coulomb pseudopotential parameter μ^* ranging from 0.1 to 0.13.[57] The calculated T_c values, along with the EPC parameter λ and the phonon frequency logarithmic average ω_{log} are presented in Fig. 5 and Table I. For $AlTiH_6$, the calculated EPC parameter λ is 1.15 and the phonon frequency logarithmic average ω_{log} is 423 K. This results in a T_c of 32–36 K at 20 GPa. $AlZrH_6$ and $AlHfH_6$ exhibit stronger EPC interactions, with

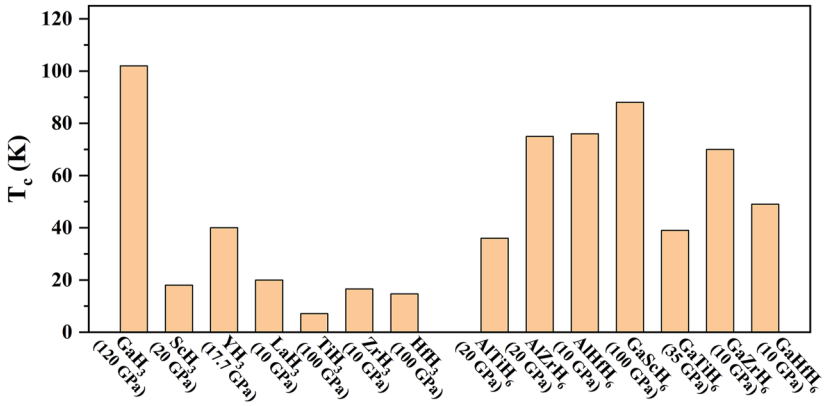

FIG. 5. Estimated T_c of the predicted A15 AMH_6 using the Allen–Dynes modified McMillan equation and those of the already known $A(M)H_3$ compounds extracted from the literature.[38–40,43–45]

TABLE I. Calculated values of the EPC parameter λ, phonon frequency logarithmic average ω_{log}, critical temperature T_c (μ^* = 0.1–0.13) using the Allen–Dynes modified McMillan equation without and with strong-coupling and shape corrections for $Pm\bar{3}$ ternary hydrides.

Phase	Pressure (GPa)	λ	ω_{log}	T_c (K), μ^* = 0.1–0.13	T_c (K) with f_1 and f_2, μ^* = 0.1–0.13
$AlTiH_6$	20	1.15	423	32–36	
$AlZrH_6$	20	1.72	494	59–64	68–75
	30	1.18	667	52–59	
$AlHfH_6$	10	2.18	397	57–60	70–76
	20	1.28	596	52–58	
$GaScH_6$	100	1.56	641	69–76	79–88
	120	1.09	890	71–62	
$GaTiH_6$	35	1.17	448	34–39	
	100	0.68	887	29–22	
$GaZrH_6$	10	1.80	438	54–58	63–70
	80	0.81	898	43–35	
$GaHfH_6$	10	1.42	454	45–49	
	86	0.74	802	32–25	

λ of 1.72 and 2.18, and the T_c values are estimated to be 59–64 and 57–60 K at 20 and 10 GPa, respectively. Considering that the λ values are higher than 1.5, the calculated T_c values are further rectified with strong-coupling (f_1) and shape (f_2) corrections and improved to 68–75 and 70–76 K, respectively. The T_c values obtained for $AlMH_6$ are indeed higher than those of AlH_3 and the corresponding MH_3 compounds.[37,39,40,45] Similarly, $GaScH_6$ exhibits the highest T_c among the studied hydrides, reaching a range of 79–88 K at a higher pressure of 100 GPa, However, its T_c is slightly lower than that of GaH_3, which has a T_c of 102 K at 120 GPa. $GaTiH_6$ has a lower T_c range of 34–39 K at 35 GPa compared with the T_c of 63–70 K for $GaZrH_6$ and 45–49 K for $GaHfH_6$ at 10 GPa.

The evolution of T_c with pressure was also investigated for $Pm\bar{3}$ AMH_6. For $AlZrH_6$, the calculated EPC parameter λ decreased from 1.72 at 20 GPa to 1.18 at 30 GPa, while ω_{log} increased from 494 to 667 K, resulting in a slight decrease in T_c with μ^* of 0.1 from 64 to 59 K (Allen–Dynes modified McMillan equation). Similarly, as the pressure increased from 10 to 20 GPa, the λ of $AlHfH_6$ decreased from 2.18 to 1.28 and the ω_{log} increased from 397 to 596 K. As a result, the calculated T_c with μ^* of 0.1 decreased slightly from 60 to 58 K. The increase in pressure leads to a stiffening of the phonon modes, which results in a decrease in the EPC parameter and an increase in ω_{log}. This compensating effect prevents a significant reduction in T_c. In addition, the T_c values of $GaMH_6$ compounds decrease with increasing pressure, owing to the competition between the decreasing EPC parameter λ and the increasing phonon frequency logarithmic average ω_{log}. Of the $Fm\bar{3}m$-like ternary hydrides, $Pmmn$ $AlScH_6$, $P4/mmm$ $AlScH_6$, and $I4/mmm$ $AlYH_6$ are found to be metallic (Fig. S19, supplementary material), and subsequent EPC calculations suggest that they exhibit superconductivity. The T_c values of these hydrides are estimated to be 42, 32, and 52 K at pressures of 80, 200, and 60 GPa, respectively (Table S3, supplementary material).

IV. CONCLUSIONS

We have carried out crystal structural predictions and first-principles calculations on alloy hydrides with the AMH_6 composition under pressure. Seven ternary hydrides, $AlMH_6$ (M = Ti, Zr, or Hf) and $GaMH_6$ (M = Sc, Ti, Zr, or Hf) were predicted to adopt the A15-type structure, and the calculated enthalpy curves indicated that the A15-type $AlMH_6$ are stable within specific pressure ranges of 92–113, 40–150 and 30–181, respectively. The pressures for onset of stability for $AlZrH_6$ and $AlHfH_6$ are lower than the stability threshold of 73 GPa for AlH_3. Phonon calculations demonstrated that A15-type $AlTiH_6$, $AlZrH_6$, and $AlHfH_6$ can be dynamically stable at relatively low pressures, such as 18, 13, and 6 GPa, respectively. Additionally, the addition of Ti, Zr, and Hf into AlH_3 influenced the position of the Fermi level, resulting in improved metallicity compared with AlH_3. Consequently, the ternary hydrides exhibited higher T_c of 36, 75, and 76 K at 20, 20, and 10 GPa, respectively. The A15-type $GaMH_6$ hydrides ($GaScH_6$, $GaTiH_6$, $GaZrH_6$, and $GaHfH_6$) were found to have minimum pressure thresholds for thermodynamic stability at 116, 95, 80, and 86 GPa, respectively, which are significantly lower than the stability threshold of 160 GPa for GaH_3. Additionally, dynamical stability calculations indicated their potential retention down to lower pressures of 97, 28, 5, and 6 GPa, respectively. EPC calculations revealed that A15-type $GaMH_6$ hydrides are superconducting, with T_c of 88, 39, 70, and 49 K at 100, 35, 10, and 10 GPa, respectively. $AlScH_6$ and $AlYH_6$ were predicted to be stable in $Fm\bar{3}m$ $Sc(Y)H_3$-like structures under pressure. The estimated T_c values for $Pmmn$, $P4/mmm$ $AlScH_6$, and $I4/mmm$ $AlYH_6$ were 42, 32, and 52 K at 80, 200, and 60 GPa, respectively. These findings suggest that alloying holds promise as a route to lower the stabilization pressure of hydrides, enabling the exploration of high-T_c hydride superconductors that can be stable at lower or ambient pressures.

SUPPLEMENTARY MATERIAL

See the supplementary material for the predicted structures of $GaTiH_6$, $GaScH_6$, $AlScH_6$, $AlYH_6$, $AlLaH_6$, $GaYH_6$, and $GaLaH_6$; ELFs; the relative enthalpy curves of $AlTiH_6$, $AlScH_6$, $AlYH_6$, $AlLaH_6$, $GaYH_6$, and $GaLaH_6$; the formation enthalpies of hydrides with higher H content in the Al–Zr–H, Ga–Sc–H, Ga–Zr–H, and Ga–Hf–H system with respect to decomposition into $AH_3 + BH_3 + H_2$ or $AMH_6 + H_2$ at 200 and 300 GPa; the relative internal energies ΔU and the ΔPV components of the enthalpy for the A15 ternary hydrides; the evolution of frequency with pressure for the studied hydrides; phonon spectra, electronic density of states, and structural information; Bader charge analyses; and superconductivity of *Pmmn* and *P*4/*mmm* $AlScH_6$ and of *I*4/*mmm* $AlYH_6$.

ACKNOWLEDGMENTS

This work was supported by the Natural Science Foundation of China (Grant Nos. 52022089, 52372261, 52288102, and 11964026), the National Key R&D Program of China (Grant No. 2022YFA1402300), the Natural Science Foundation of Hebei Province (Grant No. E2022203109), the Doctoral Fund of Henan University of Technology (Grant No. 31401579). P.L. thanks the Science and Technology Leading Talents and Innovation Team Building Projects of the Inner Mongolia Autonomous Region (Grant No. GXKY22060). A.B. acknowledges financial support from the Spanish Ministry of Science and Innovation (Grant No. FIS2019-105488GB-I00) and the Department of Education, Universities and Research of the Basque Government and the University of the Basque Country (Grant No. IT1707-22). E.Z. acknowledges the National Science Foundation (Grant No. DMR-2136038) for financial support.

AUTHOR DECLARATIONS

Conflict of Interest

The authors have no conflicts to disclose.

Author Contributions

Xiaowei Liang: Conceptualization (equal); Data curation (equal); Formal analysis (equal); Writing – original draft (equal); Writing – review & editing (equal). **Xudong Wei**: Data curation (equal); Methodology (equal). **Eva Zurek**: Writing – review & editing (supporting). **Aitor Bergara**: Writing – review & editing (supporting). **Peifang Li**: Writing – review & editing (equal). **Guoying Gao**: Conceptualization (lead); Formal analysis (lead); Funding acquisition (lead); Investigation (lead); Supervision (lead); Writing – review & editing (lead). **Yongjun Tian**: Conceptualization (equal); Funding acquisition (equal); Supervision (equal); Writing – review & editing (equal).

DATA AVAILABILITY

The data that support the findings of this study are available from the corresponding author upon reasonable request.

REFERENCES

[1] J. A. Flores-Livas, L. Boeri, A. Sanna, G. Profeta, R. Arita, and M. Eremets, "A perspective on conventional high-temperature superconductors at high pressure: Methods and materials," Phys. Rep. **856**, 1 (2020).

[2] D. V. Semenok, I. A. Kruglov, I. A. Savkin, A. G. Kvashnin, and A. R. Oganov, "On distribution of superconductivity in metal hydrides," Curr. Opin. Solid State Mater. Sci. **24**, 100808 (2020).

[3] H. Wang, X. Li, G. Gao, Y. Li, and Y. Ma, "Hydrogen-rich superconductors at high pressures," Wiley Interdiscip. Rev.: Comput. Mol. Sci. **8**, e1330 (2018).

[4] K. P. Hilleke and E. Zurek, "Tuning chemical precompression: Theoretical design and crystal chemistry of novel hydrides in the quest for warm and light superconductivity at ambient pressures," J. Appl. Phys. **131**, 070901 (2022).

[5] G. Gao, L. Wang, M. Li, J. Zhang, R. T. Howie, E. Gregoryanz, V. V. Struzhkin, L. Wang, and J. S. Tse, "Superconducting binary hydrides: Theoretical predictions and experimental progresses," Mater. Today Phys. **21**, 100546 (2021).

[6] M. I. Eremets, V. S. Minkov, A. P. Drozdov, P. P. Kong, V. Ksenofontov, S. I. Shylin, S. L. Bud'ko, R. Prozorov, F. F. Balakirev, D. Sun *et al.*, "High-temperature superconductivity in hydrides: Experimental evidence and details," J Supercond. Nov. Magn. **35**, 965 (2022).

[7] A. P. Drozdov, M. I. Eremets, I. A. Troyan, V. Ksenofontov, and S. I. Shylin, "Conventional superconductivity at 203 kelvin at high pressures in the sulfur hydride system," Nature **525**, 73 (2015).

[8] M. Einaga, M. Sakata, T. Ishikawa, K. Shimizu, M. I. Eremets, A. P. Drozdov, I. A. Troyan, N. Hirao, and Y. Ohishi, "Crystal structure of the superconducting phase of sulfur hydride," Nat. Phys. **12**, 835 (2016).

[9] A. P. Drozdov, P. P. Kong, V. S. Minkov, S. P. Besedin, M. A. Kuzovnikov, S. Mozaffari, L. Balicas, F. F. Balakirev, D. e. Graf, V. B. Prakapenka *et al.*, "Superconductivity at 250 K in lanthanum hydride under high pressures," Nature **569**, 528 (2019).

[10] M. Somayazulu, M. Ahart, A. K. Mishra, Z. M. Geballe, M. Baldini, Y. Meng, V. V. Struzhkin, and R. J. Hemley, "Evidence for superconductivity above 260 K in lanthanum superhydride at megabar pressures," Phys. Rev. Lett. **122**, 027001 (2019).

[11] D. V. Semenok, A. G. Kvashnin, A. G. Ivanova, V. Svitlyk, V. Yu. Fominski, A. V. Sadakov, O. A. Sobolevskiy, V. M. Pudalov, I. A. Troyan, and A. R. Oganov, "Superconductivity at 161 K in thorium hydride ThH_{10}: Synthesis and properties," Mater. Today **33**, 36 (2020).

[12] I. A. Troyan, D. V. Semenok, A. G. Kvashnin, A. V. Sadakov, O. A. Sobolevskiy, V. M. Pudalov, A. G. Ivanova, V. B. Prakapenka, E. Greenberg, A. G. Gavriliuk *et al.*, "Anomalous high-temperature superconductivity in YH_6," Adv. Mater. **33**, 2006832 (2021).

[13] P. Kong, V. S. Minkov, M. A. Kuzovnikov, A. P. Drozdov, S. P. Besedin, S. Mozaffari, L. Balicas, F. F. Balakirev, V. B. Prakapenka, S. Chariton *et al.*, "Superconductivity up to 243 K in the yttrium-hydrogen system under high pressure," Nat. Commun. **12**, 5075 (2021).

[14] E. Snider, N. Dasenbrock-Gammon, R. McBride, X. Wang, N. Meyers, K. V. Lawler, E. Zurek, A. Salamat, and R. P. Dias, "Synthesis of yttrium superhydride superconductor with a transition temperature up to 262 K by catalytic hydrogenation at high pressures," Phys. Rev. Lett. **126**, 117003 (2021).

[15] L. Ma, K. Wang, Y. Xie, X. Yang, Y. Wang, M. Zhou, H. Liu, X. Yu, Y. Zhao, H. Wang *et al.*, "High-temperature superconducting phase in clathrate calcium hydride CaH_6 up to 215 K at a pressure of 172 GPa," Phys. Rev. Lett. **128**, 167001 (2022).

[16] Z. Li, X. He, C. Zhang, X. Wang, S. Zhang, Y. Jia, S. Feng, K. Lu, J. Zhao, J. Zhang *et al.*, "Superconductivity above 200 K discovered in superhydrides of calcium," Nat. Commun. **13**, 2863 (2022).

[17] D. V. Semenok, I. A. Troyan, A. G. Ivanova, A. G. Kvashnin, I. A. Kruglov, M. Hanfland, A. V. Sadakov, O. A. Sobolevskiy, K. S. Pervakov, I. S. Lyubutin *et al.*, "Superconductivity at 253 K in lanthanum–yttrium ternary hydrides," Mater. Today **48**, 18 (2021).

[18] J. Bi, Y. Nakamoto, P. Zhang, Y. Wang, L. Ma, Y. Wang, B. Zou, K. Shimizu, H. Liu, M. Zhou *et al.*, "Stabilization of superconductive La–Y alloy superhydride with T_c above 90 K at megabar pressure," Mater. Today Phys. **28**, 100840 (2022).

[19]J. Bi, Y. Nakamoto, P. Zhang, K. Shimizu, B. Zou, H. Liu, M. Zhou, G. Liu, H. Wang, and Y. Ma, "Giant enhancement of superconducting critical temperature in substitutional alloy (La,Ce)H_9," Nat. Commun. **13**, 5952 (2022).
[20].S. Chen, Y. Qian, X. Huang, W. Chen, J. Guo, K. Zhang, J. Zhang, H. Yuan, and T. Cui, "High-temperature superconductivity up to 223 K in the Al stabilized metastable hexagonal lanthanum superhydride," Natl. Sci. Rev (published online) (2023).
[21]X. Li, X. Huang, D. Duan, C. J. Pickard, D. Zhou, H. Xie, Q. Zhuang, Y. Huang, Q. Zhou, B. Liu, and T. Cui, "Polyhydride CeH_9 with an atomic-like hydrogen clathrate structure," Nat. Commun. **10**, 3461 (2019).
[22]N. P. Salke, M. M. Davari Esfahani, Y. Zhang, I. A. Kruglov, J. Zhou, Y. Wang, E. Greenberg, V. B. Prakapenka, J. Liu, A. R. Oganov, and J.-F. Lin, "Synthesis of clathrate cerium superhydride CeH_9 at 80-100 GPa with atomic hydrogen sublattice," Nat. Commun. **10**, 4453 (2019).
[23]H. Wang, J. S. Tse, K. Tanaka, T. Iitaka, and Y. Ma, "Superconductive sodalite-like clathrate calcium hydride at high pressures," Proc. Natl. Acad. Sci. U. S. A. **109**, 6463 (2012).
[24]Y. Li, J. Hao, H. Liu, J. S. Tse, Y. Wang, and Y. Ma, "Pressure-stabilized superconductive yttrium hydrides," Sci. Rep. **5**, 9948 (2015).
[25]H. Liu, I. I. Naumov, R. Hoffmann, N. W. Ashcroft, and R. J. Hemley, "Potential high- *Tc* superconducting lanthanum and yttrium hydrides at high pressure," Proc. Natl. Acad. Sci. U. S. A. **114**, 6990 (2017).
[26]F. Peng, Y. Sun, C. J. Pickard, R. J. Needs, Q. Wu, and Y. Ma, "Hydrogen clathrate structures in rare earth hydrides at high pressures: Possible route to room-temperature superconductivity," Phys. Rev. Lett. **119**, 107001 (2017).
[27]X. Liang, A. Bergara, L. Wang, B. Wen, Z. Zhao, X.-F. Zhou, J. He, G. Gao, and Y. Tian, "Potential high-T_c superconductivity in $CaYH_{12}$ under pressure," Phys. Rev. B **99**, 100505 (2019).
[28]T. Ishikawa, T. Miyake, and K. Shimizu, "Materials informatics based on evolutionary algorithms: Application to search for superconducting hydrogen compounds," Phys. Rev. B **100**, 174506 (2019).
[29]X. Liang, A. Bergara, X. Wei, X. Song, L. Wang, R. Sun, H. Liu, R. J. Hemley, L. Wang, G. Gao, and Y. Tian, "Prediction of high-T_c superconductivity in ternary lanthanum borohydrides," Phys. Rev. B **104**, 134501 (2021).
[30]Z. Zhang, T. Cui, M. J. Hutcheon, A. M. Shipley, HM. SongDu, V. Z. Kresin, D. Duan, C. J. Pickard, and Y. Yao, "Design principles for high-temperature superconductors with a hydrogen-based alloy backbone at moderate pressure," Phys. Rev. Lett. **128**, 047001 (2022).
[31]S. Di Cataldo, C. Heil, W. von der Linden, and L. Boeri, "$LaBH_8$: Towards high-T_c low-pressure superconductivity in ternary superhydrides," Phys. Rev. B **104**, L020511 (2021).
[32]R. Lucrezi, S. Di Cataldo, W. von der Linden, L. Boeri, and C. Heil, "In-silico synthesis of lowest-pressure high-*T*c ternary superhydrides," npj Comput. Mater. **8**, 119 (2022).
[33]Y. Sun, S. Sun, X. Zhong, and H. Liu, "Prediction for high superconducting ternary hydrides below megabar pressure," J. Phys.: Condens. Matter **34**, 505404 (2022).
[34]M. Gao, X.-W. Yan, Z.-Y. Lu, and T. Xiang, "Phonon-mediated high-temperature superconductivity in the ternary borohydride KB_2H_8 under pressure near 12 GPa," Phys. Rev. B **104**, L100504 (2021).
[35]M.-J. Jiang, Y.-L. Hai, H.-L. Tian, H.-B. Ding, Y.-J. Feng, C.-L. Yang, X.-J. Chen, and G.-H. Zhong, "High-temperature superconductivity below 100 GPa in ternary C-based hydride MC_2H_8 with molecular crystal characteristics (M=Na, K, Mg, Al, and Ga)," Phys. Rev. B **105**, 104511 (2022).
[36]C. J. Pickard and R. J. Needs, "Metallization of aluminum hydride at high pressures: A first-principles study," Phys. Rev. B **76**, 144114 (2007).
[37]I. Goncharenko, M. I. Eremets, M. Hanfland, J. S. Tse, M. Amboage, Y. Yao, and I. A. Trojan, "Pressure-induced hydrogen-dominant metallic state in aluminum hydride," Phys. Rev. Lett. **100**, 045504 (2008).
[38]G. Gao, H. Wang, A. Bergara, Y. Li, G. Liu, and Y. Ma, "Metallic and superconducting gallane under high pressure," Phys. Rev. B **84**, 064118 (2011).
[39]H. Xie, W. Zhang, D. Duan, X. Huang, Y. Huang, H. Song, X. Feng, Y. Yao, C. J. Pickard, and T. Cui, "Superconducting zirconium polyhydrides at moderate pressures," J. Phys. Chem. Lett. **11**, 646 (2020).
[40]H. Xie, Y. Yao, X. Feng, D. Duan, H. Song, Z. Zhang, S. Jiang, S. A. T. Redfern, V. Z. Kresin, C. J. Pickard, and T. Cui, "Hydrogen pentagraphenelike structure stabilized by hafnium: A high-temperature conventional superconductor," Phys. Rev. Lett. **125**, 217001 (2020).
[41]B. Rousseau and A. Bergara, "Giant anharmonicity suppresses superconductivity in AlH_3 under pressure," Phys. Rev. B **82**, 104504 (2010).
[42]X. Ye, R. Hoffmann, and N. W. Ashcroft, "Theoretical study of phase separation of scandium hydrides under high pressure," J. Phys. Chem. C **119**, 5614 (2015).
[43]D. Y. Kim, R. H. Scheicher, H.-k. Mao, T. W. Kang, and R. Ahuja, "General trend for pressurized superconducting hydrogen-dense materials," Proc. Natl. Acad. Sci. U. S. A. **107**, 2793 (2010).
[44]D. Y. Kim, R. H. Scheicher, and R. Ahuja, "Predicted high-temperature superconducting state in the hydrogen-dense transition-metal hydride YH_3 at 40 K and 17.7 GPa," Phys. Rev. Lett. **103**, 077002 (2009).
[45]J. Zhang, J. M. McMahon, A. R. Oganov, X. Li, X. Dong, H. Dong, and S. Wang, "High-temperature superconductivity in the Ti-H system at high pressures," Phys. Rev. B **101**, 134108 (2020).
[46]G. R. Stewart, "Superconductivity in the A15 structure," Physica C **514**, 28 (2015).
[47]X. X. WeiHao, A. Bergara, E. Zurek, X. Liang, L. Wang, X. Song, P. Li, L. Wang, G. Gao, and Y. Tian, "Designing ternary superconducting hydrides with A15-type structure at moderate pressures," Mater. Today Phys. **34**, 101086 (2023).
[48]W. Zhao, H. Song, M. Du, Q. Jiang, T. Ma, M. Xu, D. Duan, and T. Cui, "Pressure-induced high-temperature superconductivity in ternary Y–Zr–H compounds," Phys. Chem. Chem. Phys. **25**, 5237 (2023).
[49]Y. Wang, J. Lv, L. Zhu, and Y. Ma, "Crystal structure prediction via particle-swarm optimization," Phys. Rev. B **82**, 094116 (2010).
[50]Y. Wang, J. Lv, L. Zhu, and Y. Ma, "CALYPSO: A method for crystal structure prediction," Comput. Phys. Commun. **183**, 2063 (2012).
[51]G. Kresse and J. Furthmüller, "Efficient iterative schemes for *ab initio* total-energy calculations using a plane-wave basis set," Phys. Rev. B **54**, 11169 (1996).
[52]J. P. Perdew, K. Burke, and M. Ernzerhof, "Generalized gradient approximation made simple," Phys. Rev. Lett. **77**, 3865 (1996).
[53]P. E. Blöchl, "Projector augmented-wave method," Phys. Rev. B **50**, 17953 (1994).
[54]A. Togo, F. Oba, and I. Tanaka, "First-principles calculations of the ferroelastic transition between rutile-type and $CaCl_2$-type SiO_2 at high pressures," Phys. Rev. B **78**, 134106 (2008).
[55]P. Giannozzi, S. Baroni, N. Bonini, M. Calandra, R. Car, C. Cavazzoni, D. Ceresoli, G. L. Chiarotti, M. Cococcioni, I. Dabo, A. Dal Corso, S. de Gironcoli, S. Fabris, G. Fratesi, R. Gebauer, U. Gerstmann, C. Gougoussis, A. Kokalj, M. Lazzeri, L. Martin-Samos, N. Marzari, F. Mauri, R. Mazzarello, S. Paolini, A. Pasquarello, L. Paulatto, C. Sbraccia, S. Scandolo, G. Sclauzero, A. P. Seitsonen, A. Smogunov, P. Umari, and R. M. Wentzcovitch, "QUANTUM ESPRESSO: A modular and open-source software project for quantum simulations of materials," J. Phys.: Condens. Matter **21**, 395502 (2009).
[56]R. Bader, *Atoms in Molecules: A Quantum Theory* (Oxford University Press, Oxford, 1994).
[57]P. B. Allen and R. C. Dynes, "Transition temperature of strong-coupled superconductors reanalyzed," Phys. Rev. B **12**, 905 (1975).